Magic wavelengths for the *np*-*ns* transitions in alkali-metal atoms

Bindiya Arora and M. S. Safronova
Department of Physics and Astronomy, University of Delaware, Newark, Delaware 19716-2593, USA

Charles W. Clark
Physics Laboratory, National Institute of Standards and Technology, Technology Administration, U.S. Department of Commerce, Gaithersburg, Maryland 20899-8410, USA

(Received 2 September 2007; published 15 November 2007)

Extensive calculations of the electric-dipole matrix elements in alkali-metal atoms are conducted using the relativistic all-order method. This approach is a linearized version of the coupled-cluster method, which sums infinite sets of many-body perturbation theory terms. All allowed transitions between the lowest ns, $np_{1/2}$, $np_{3/2}$ states and a large number of excited states are considered in these calculations and their accuracy is evaluated. The resulting electric-dipole matrix elements are used for the high-precision calculation of frequency-dependent polarizabilities of the excited states of alkali-metal atoms. We find "magic" wavelengths in alkali-metal atoms for which the ns and $np_{1/2}$ and $np_{3/2}$ atomic levels have the same ac Stark shifts, which facilitates state-insensitive optical cooling and trapping.

DOI: 10.1103/PhysRevA.76.052509 PACS number(s): 32.10.Dk, 32.80.Pj, 31.15.Dv, 32.70.Jz

I. INTRODUCTION

Recent progress in the manipulation of neutral atoms in optical dipole traps offers advancement in a wide variety of applications. One such application is toward the quantum computational scheme, which realizes qubits as the internal states of trapped neutral atoms [1]. In this scheme, it is essential to precisely localize and control neutral atoms with minimum decoherence. Other applications include the next generation of atomic clocks, which may attain relative uncertainty of 10^{-18}, enabling new tests of fundamental physics, more accurate measurements of fundamental constants and their time dependence, further improvement of global positioning system measurements, etc.

In a far-detuned optical dipole trap, the potential experienced by an atom can be either attractive or repulsive depending on the sign of the frequency-dependent Stark shift (ac Stark shift) due to the trap light. The excited states may experience an ac Stark shift with an opposite sign of the ground state Stark shift, affecting the fidelity of the experiments. A solution to this problem was proposed by Katori *et al.* [2], who suggested that the laser can be tuned to a magic wavelength λ_{magic}, where lattice potentials of equal depth are produced for the two electronic states of the clock transition. In their experiment, they demonstrated that a λ_{magic} exists for the $^1S_0$-$^3P_0$ clock transition of ^{87}Sr in an optical lattice. Four years later, McKeever *et al.* [3] demonstrated state-insensitive trapping of Cs atoms at $\lambda_{\text{magic}} \approx 935$ nm while still maintaining a strong coupling for the $6p_{3/2}$-$6s_{1/2}$ transition. The ability to trap neutral atoms inside high-Q cavities in the strong coupling regime is of particular importance to the quantum computation and communication schemes [3].

In this paper, we evaluate the magic wavelengths in Na, K, Rb, and Cs atoms for which the ns ground state and either of the first two np_j excited states experience the same optical potential for state-insensitive cooling and trapping. We accomplish this by matching the ac polarizabilities of the atomic ns and np_j states. We conduct extensive calculations of the relevant electric-dipole matrix elements using the relativistic all-order method and evaluate the uncertainties of the resulting ac polarizabilities. We also study the ac Stark shifts of these atoms to determine the dependence of λ_{magic} on their hyperfine structure.

The paper is organized as follows. In Sec. II, we give a short description of the method used for the calculation of the ac polarizabilities and list our results for scalar and tensor ac polarizabilities. In Sec. III, we discuss the effect of ac Stark shifts on the hyperfine structure of the alkali-metal atoms. In Sec. IV, we discuss the magic wavelength results for each of the atoms considered in this work.

II. DYNAMIC POLARIZABILITIES

We begin with an outline of calculations of the ac Stark shift for linearly polarized light, following Refs. [4,5]. Angels and Sandars [4] discussed the methodology for the calculation of the Stark shift and parametrization of the Stark shift in terms of the scalar and tensor polarizabilities. Stark shifts are obtained as the energy eigenvalues of the Schrödinger equation with interaction operator V_{I} given by

$$V_{\text{I}} = -\vec{\epsilon}\cdot\vec{d}, \tag{1}$$

where $\vec{\epsilon}$ is the applied external electric field and $\vec{d}$ is the electric-dipole operator. The first-order shift associated with V_{I} vanishes in alkali-metal atoms. Therefore, the Stark shift ΔE of level v is calculated from the second-order expression

$$\Delta E = \sum_k \frac{\langle j_v m_v|V_{\text{I}}|j_k m_k\rangle\langle j_k m_k|V_{\text{I}}|j_v m_v\rangle}{E_v - E_k}, \tag{2}$$

where the sum over k includes all intermediate states allowed by electric-dipole transition selection rules, and E_k is the energy of the state k.

Using the Wigner-Eckart theorem, one finds that ΔE can be written as the sum [6]

$$\Delta E = -\frac{1}{2}\alpha_0(\omega)\epsilon^2 - \frac{1}{2}\alpha_2(\omega)\frac{3m_j^2 - j_v(j_v+1)}{j_v(2j_v-1)}\epsilon^2, \quad (3)$$

where $\alpha_0(\omega)$ and $\alpha_2(\omega)$ are the scalar and tensor ac polarizabilities, respectively, of an atomic state v. The laser frequency ω is assumed to be several linewidths off-resonance. Here, the polarization vector of the light defines the z direction.

The scalar ac polarizability $\alpha_0(\omega)$ of an atom can be further separated into an ionic core contribution $\alpha_{\text{core}}(\omega)$ and a valence contribution $\alpha_0^v(\omega)$. The core contribution has a weak dependence on the frequency for the values of ω relevant to this work. Therefore, we use the static ionic core polarizability values calculated using the random-phase approximation (RPA) in Ref. [7]. The valence contribution $\alpha_0^v(\omega)$ to the static polarizability of a monovalent atom in a state v is given by [8]

$$\alpha_0^v(\omega) = \frac{2}{3(2j_v+1)}\sum_k \frac{\langle k\|d\|v\rangle^2(E_k - E_v)}{(E_k - E_v)^2 - \omega^2}, \quad (4)$$

where $\langle k\|d\|v\rangle$ is the reduced electric-dipole ($E1$) matrix element. The experimental energies E_i of the most important states i which contribute to this sum have been compiled for the alkali atoms in Refs. [9–11]. Unless stated otherwise, we use atomic units (a.u.) for all matrix elements and polarizabilities throughout this paper: the numerical values of the elementary charge e, the reduced Planck constant $\hbar = h/2\pi$, and the electron mass m_e are set equal to 1. The atomic unit for polarizability can be converted to SI units via α/h $[\text{Hz}/(\text{V}/\text{m})^2] = 2.48832 \times 10^{-8}\alpha$ (a.u.), where the conversion coefficient is $4\pi\epsilon_0 a_0^3/h$ and the Planck constant h is factored out.

The tensor ac polarizability $\alpha_2(\omega)$ is given by [12]

$$\alpha_2(\omega) = -4C\sum_k (-1)^{j_v+j_k+1}\begin{Bmatrix} j_v & 1 & j_k \\ 1 & j_v & 2 \end{Bmatrix} \times \frac{\langle k\|d\|v\rangle^2(E_k - E_v)}{(E_k - E_v)^2 - \omega^2},$$

$$C = \left(\frac{5j_v(2j_v-1)}{6(j_v+1)(2j_v+1)(2j_v+3)}\right)^{1/2}. \quad (5)$$

The ground-state ac polarizabilities of alkali-metal atoms have been calculated to high precision [13]. However, no accurate systematic study of the ac polarizabilities of the excited states of alkali-metal atoms is currently available. The polarizability calculations for the excited np states are relatively complicated because in addition to p-s transitions they also involve p-d transition matrix elements. The matrix elements involving the nd states are generally more difficult to evaluate accurately, especially for the heavier alkalies.

In this work, we calculate np-$n'd$ transition matrix elements using the relativistic all-order method [14,15] and use these values to accurately determine the $np_{1/2}$ and $np_{3/2}$ state ac polarizabilities. In the relativistic all-order method, all single and double (SD) excitations of the Dirac-Fock (DF) wave function are included to all orders of perturbation theory. For some matrix elements, we found it necessary to also include single, double, and partial triple (SDpT) excitations into the wave functions (SDpT method). We conduct additional semi-empirical scaling of our all-order SD and SDpT values where we expect scaled values to be more accurate or for more accurate evaluation of the uncertainties. The scaling procedure has been described in Refs. [8,15,16].

We start the calculation of the np state valence polarizabilities using Eqs. (4) and (5). For the wavelength range considered in this work, the first few terms in the sums over k give the dominant contributions. Therefore, we can separate the np state valence polarizability into a main part α_{main} that includes these dominant terms, and a remainder α_{tail}. We use a complete set of DF wave functions on a nonlinear grid generated using B-splines [17] in all our calculations. We use 70 splines of order 11 for each value of the angular momentum. A cavity radius of 220 a.u. is chosen to accommodate all valence orbitals of α_{main}. In our K and Rb calculations, we include all ns states up to $10s$ and all nd states up to $9d$; $11s$, $12s$, and $10d$ are also added for Cs. Such a large number of states is needed to reduce uncertainties in the remainder α_{tail}. We use the experimental values compiled in Ref. [18] along with their uncertainties for the first np-ns matrix elements, for example, the $5p_j$-$5s$ matrix elements in Rb. We use the SD scaled values for some of the np-$n'd$ and np-$n's$ matrix elements in the cases where it was essential to reduce the uncertainty of our calculations and where the scaling is expected to produce more accurate results based on the type of the dominant correlation corrections. This issue is discussed in detail in Refs. [19,20] and references therein.

In Table I, we give the contributions to the scalar and tensor polarizabilities of the Rb $5p_{3/2}$ state at 790 nm to illustrate the details of the calculation. The absolute values of the corresponding reduced electric-dipole matrix elements d used in the calculations are also given. The contributions from the main term are listed separately. We also list the resonant wavelengths λ_{res} corresponding to each transition to illustrate which transitions are close to 790 nm. As noted above, we use the experimental values for the $5p_{3/2}$-$5s$ matrix element from the Ref. [18]. We use the recommended values for the $5p_{3/2}$-$4d_j$ transitions derived from the Stark shift measurements [21] in Ref. [22]. We find that the contribution of the $5p_{3/2}$-$5s$ transition is dominant since the wavelength of this transition ($\lambda_{\text{res}} = 780$ nm) is the closest to the laser wavelength. The next dominant contribution for the scalar polarizability is from the $5p_{3/2}$-$5d_{5/2}$ transition ($\lambda_{\text{res}} = 776$ nm). While the contribution from this transition is less than one tenth of the dominant contributions, it gives the dominant contribution to the final uncertainty owing to a very large correlation correction to the $5p_{3/2}$-$5d_{5/2}$ reduced electric-dipole matrix element. In fact, the lowest-order DF value for this transition is only 0.493 a.u. while our final (SD scaled) value is 1.983 a.u. We take the uncertainty in this transition to be the maximum difference of our final values and *ab initio* SDpT and scaled SDpT values. While the $5p_{3/2}$-$5d_{3/2}$ transition has almost the same transition wavelength owing to the very small fine-structure splitting of the $5d$ state, the corresponding contribution is nine times smaller owing to the fact that the $5p_{3/2}$-$5d_{3/2}$ reduced electric-dipole matrix element is smaller than the $5p_{3/2}$-$5d_{5/2}$ matrix element

TABLE I. Contributions to the $5p_{3/2}$ scalar (α_0) and tensor (α_2) polarizabilities at $\lambda=790$ nm in Rb and their uncertainties in units of a_0^3. The absolute values of corresponding reduced electric-dipole matrix elements d (in ea_0) and the corresponding transition wavelength in vacuum λ_{res} (in nm) are also given.

Contribution	λ_{res}	d	α_0	α_2
$5p_{3/2}$-$5s_{1/2}$	780	5.977	−4153(5)	4153(5)
$5p_{3/2}$-$6s_{1/2}$	1367	6.047	−92(1)	92(1)
$5p_{3/2}$-$7s_{1/2}$	741	1.350	41.1(1)	−41.1(1)
$5p_{3/2}$-$8s_{1/2}$	616	0.708	2.88(2)	−2.88(2)
$5p_{3/2}$-$9s_{1/2}$	566	0.466	0.922(6)	−0.922(6)
$5p_{3/2}$-$10s_{1/2}$	539	0.341	0.430(3)	−0.430(3)
$5p_{3/2}$-$4d_{3/2}$	1529	3.633	−26.9(4)	−21.5(4)
$5p_{3/2}$-$5d_{3/2}$	776	0.665	36(3)	29(3)
$5p_{3/2}$-$6d_{3/2}$	630	0.506	1.6(3)	1.3(3)
$5p_{3/2}$-$7d_{3/2}$	573	0.370	0.60(9)	0.48(7)
$5p_{3/2}$-$8d_{3/2}$	543	0.283	0.30(4)	0.24(3)
$5p_{3/2}$-$9d_{3/2}$	526	0.225	0.18(2)	0.14(2)
$5p_{3/2}$-$4d_{5/2}$	1529	10.899	−242(4)	48.4(8)
$5p_{3/2}$-$5d_{5/2}$	776	1.983	317(28)	−63(6)
$5p_{3/2}$-$6d_{5/2}$	630	1.512	14(3)	−2.9(6)
$5p_{3/2}$-$7d_{5/2}$	573	1.104	5.4(8)	−1.1(2)
$5p_{3/2}$-$8d_{5/2}$	543	0.845	2.7(3)	−0.54(6)
$5p_{3/2}$-$9d_{5/2}$	526	0.672	1.6(2)	−0.31(3)
α_{tail}			19(14)	−5(5)
α_{core}			9.1(5)	
Total			−4060(32)	4184(9)

by a factor of 3. As expected, the contributions from the core and tail terms are very small in comparison with the total polarizability values at this wavelength.

In Table II, we compare our results for the first excited $np_{1/2}$ and $np_{3/2}$ state static polarizabilities for Na, K, Rb, and Cs with the previous experimental and theoretical studies. The measurements of the ground state static polarizability of Na by Ekstrom *et al.* [24] were combined with the experimental Stark shifts from Refs. [25,32] to predict precise values for the $3p_{1/2}$ and $3p_{3/2}$ scalar polarizabilities [24]. The tensor polarizability of the $3p_{3/2}$ state of Na has been measured by Windholz *et al.* [25]. The Stark shift measurements for K and Rb have been carried out by Miller *et al.* [26] for $D1$ lines and by Krenn *et al.* [28] for $D2$ lines. We have combined these Stark shift measurements with the recommended ground-state polarizability values from Ref. [27] to obtain the np_j polarizability values that we quote as experimental results. The $np_{3/2}$ tensor polarizabilities in K and Rb were measured in Ref. [28]. Accurate $D1$ and $D2$ Stark shift measurements for Cs have been reported in Refs. [21,31]. The most accurate experimental measurement of the $6s$ ground-state polarizability from Ref. [30] has been used to derive the values of the $6p_{1/2}$ and $6p_{3/2}$ state polarizabilities in Cs quoted in Table II. Our results are in excellent agreement with the experimental values.

We note that we use our theoretical values for the $4p$-$3d$ transitions in K and $5p$-$4d$ transitions in Rb to establish the accuracy of our approach. We use more accurate recommended values for these transitions derived from the experimental Stark shifts [21] in Ref. [22] in all other calculations in this work, as described in the discussion of Table I.

TABLE II. Comparison of static polarizabilities of $np_{1/2}$ and $np_{3/2}$ states with other experiments and theory. Units: a_0^3.

Na	$\alpha_0(3p_{1/2})$	$\alpha_0(3p_{3/2})$	$\alpha_2(3p_{3/2})$
Present	359.9	361.6	−88.4
Other	359.7[a]	361.4[a]	−88.0[a]
Exp.	359.2(6)[b]	360.4(7)[b]	−88.3(4)[c]
K	$\alpha_0(4p_{1/2})$	$\alpha_0(4p_{3/2})$	$\alpha_2(4p_{3/2})$
Present	602	613	−109
Other	605[a]	616[a]	−111[a]
Exp.	606.7(6)[d]	614(10)[e]	−107(2)[e]
Rb	$\alpha_0(5p_{1/2})$	$\alpha_0(5p_{3/2})$	$\alpha_2(5p_{3/2})$
Present	805	867	−167
Other	807[a]	870[a]	−171[a]
Exp.	810.6(6)[d]	857(10)[e]	−163(3)[e]
Cs	$\alpha_0(6p_{1/2})$	$\alpha_0(6p_{3/2})$	$\alpha_2(6p_{3/2})$
Present	1338	1650	−261
Other	1290[f]	1600[f]	−233[f]
Exp.	1328.4(6)[g]	1641(2)[h]	−262(2)[h]

[a]Reference [23].
[b]Reference [24].
[c]Reference [25].
[d]Derived from Ref. [26], $D1$ line Stark shift measurements and recommended values for ground-state polarizability from Ref. [27].
[e]Reference [28].
[f]Reference [29].
[g]Derived from Ref. [21], $D1$ line Stark shift measurement and ground-state polarizability measurement from Ref. [30].
[h]Derived from Ref. [31], $D2$ line Stark shift measurement and ground-state polarizability from Ref. [30].

III. ac STARK EFFECT FOR HYPERFINE LEVELS

In the above discussion, we neglected the hyperfine structure of the atomic levels. However, it is essential to include the hyperfine structure which is affected by the presence of external electric field for practical applications discussed in this work. In this section, we calculate the eigenvalues of the Hamiltonian H representing the combined effect of Stark and hyperfine interactions. Then, we subtract the hyperfine splitting from the above eigenvalues to get the ac Stark shift of a hyperfine level. This value is used to calculate the ac Stark shift of the transition from a hyperfine level of the excited np state to a hyperfine level of the ground ns state.

A. Matrix elements of the Stark operator

First, we evaluate the matrix elements of Stark operator in the hyperfine basis. The energy difference between two hyperfine levels is relatively small for cases considered in this

work, and the hyperfine levels are expected to mix even if small electric fields are applied. Therefore, the Stark operator now has non-zero off-diagonal matrix elements. The general equation for the matrix elements is given by

$$\Delta E_{F,F''} = \sum_k \frac{\langle IjFM|V_{\rm I}|I_k j_k F_k M_k\rangle\langle I_k j_k F_k M_k|V_{\rm I}|I''j''F''M''\rangle}{E_v - E_k}, \tag{6}$$

where $|IjFM\rangle$ represents atomic states in hyperfine basis, I is the nuclear spin, and $\mathbf{F}=\mathbf{I}+\mathbf{j}$.

The interaction operator $V_{\rm I}$ given by Eq. (1) does not affect the nuclear spin I. In addition, the shifts due to $V_{\rm I}$ are not high enough to cause mixing between two levels with different angular momentum j. As a result, $\Delta E_{F,F''}$ is diagonal in I and j. These approximations enable us to label the states in hyperfine basis as $|FM\rangle$, and Eq. (6) can be simplified as

$$\Delta E_{F,F''} = \sum_k \frac{\langle FM|V_{\rm I}|F_k M_k\rangle\langle F_k M_k|V_{\rm I}|F''M''\rangle}{E_v - E_k}. \tag{7}$$

One can write the above matrix element as

$$\Delta E_{F,F''} = \langle FM|V_{\rm II}|F''M''\rangle, \tag{8}$$

where the Stark shift operator $V_{\rm II}$ is defined in terms of λ operator as

$$V_{\rm II} = V_{\rm I}\lambda V_{\rm I}, \tag{9}$$

$$\lambda = \sum_k \frac{|F_k M_k\rangle\langle F_k M_k|}{E_v - E_k}. \tag{10}$$

If the applied electric field is in the z direction, then the energy shifts are diagonal in M. Thus, the matrix elements can be written as

$$\Delta E_{F,F''} = \langle FM|V_{\rm II}|F''M\rangle. \tag{11}$$

We use the Wigner-Eckart theorem to carry out the angular reduction, i.e., sum over the magnetic quantum numbers. Then, the matrix elements can be written in terms of scalar and tensor polarizabilities as

$$\langle FM|V_{\rm II}|F''M\rangle = -\frac{1}{2}\alpha_0(\omega)\epsilon^2\delta_{F,F''} - \frac{1}{2}\alpha_2(\omega)\epsilon^2\langle FM|Q|F''M\rangle. \tag{12}$$

The first term in the equation above, containing the scalar polarizability, results in the equal shifts of all of the hyperfine levels and is nonzero only for the diagonal matrix elements ($F=F''$). The tensor part mixes states of different F through the Q operator. The nonzero matrix elements of Q are

$$\langle FM|Q|F''M\rangle = \left[\frac{(j+1)(2j+1)(2j+3)}{j(2j-1)}\right]^{1/2} \times (-1)^{I+j+F-F''-M}\sqrt{(2F+1)(2F''+1)} \times \begin{pmatrix} F & 2 & F'' \\ M & 0 & -M \end{pmatrix}\begin{Bmatrix} F & 2 & F'' \\ j & I & j \end{Bmatrix}. \tag{13}$$

For each magnetic sublevel, there is a matrix with rows and columns labeled by F and F''. Therefore, magnetic sublevels with different values of $|M|$ are shifted by a different amount. A detailed discussion of this matrix is given by Schmieder [5].

B. Energy eigenvalues

Since the Stark interactions considered in this work are comparable to the hyperfine interactions, we find the combined shift of a hyperfine level by diagonalizing the Hamiltonian given by

$$H = V_{\rm hfs} + V_{\rm II}, \tag{14}$$

where $V_{\rm hfs}$ is the hyperfine interaction operator. In the hyperfine basis, $V_{\rm hfs}$ is diagonal with the following matrix elements [33]:

$$\langle FM|V_{\rm hfs}|FM\rangle = \frac{1}{2}Az + \frac{3z(z+1) - 4I(I+1)j(j+1)}{4I(2I-1)2j(2j-1)}B, \tag{15}$$

where $z=F(F+1)-I(I+1)-j(j+1)$, and A and B are hyperfine-structure constants [34]. The matrix elements of H which describe the combined effect of the Stark interaction $V_{\rm II}$ and hyperfine interaction $V_{\rm hfs}$ are given by

$$V_{F,F'';M} = \langle FM|V_{\rm II}|F''M\rangle + \langle FM|V_{\rm hfs}(F=F'')|F''M\rangle. \tag{16}$$

Using Eq. (12) and Eq. (15), the above matrix elements can be reduced to a more useful form

$$V_{F,F'';M} = -\frac{1}{2}\alpha_0\epsilon^2\delta_{F,F''} - \frac{1}{2}\alpha_2\epsilon^2\langle FM|Q|F''M\rangle + \langle FM|V_{\rm hfs}(F=F'')|F''M\rangle. \tag{17}$$

The combined shift of a hyperfine level is evaluated by diagonalizing the matrix formed with $V_{F,F'';M}$. The resulting diagonal matrix element ($\Delta E_{F,F}$) corresponds to the shift in a hyperfine level F, resulting from two effects: the hfs interaction $V_{\rm hfs}$ and the Stark effect $V_{\rm II}$. Consequently, we should subtract the hyperfine splitting from the these shifts to get the ac Stark shift of a level given by

$$\Delta_{nl_jFM} = \Delta E_{F,F} - \langle FM|V_{\rm hfs}(F=F'')|F''M\rangle. \tag{18}$$

The ac Stark shift of the transition from an excited state to the ground state $\Delta E(n'l'_{j'}F'M' \rightarrow nl_jFM)$ is determined as the difference between the ac Stark shifts of the two states. We calculate the magic wavelength where the ac Stark shift of the *np-ns* transition is equal to zero. The results of the calculation are presented in the next section.

IV. MAGIC WAVELENGTHS FOR THE *np-ns* TRANSITIONS

We define the magic wavelength $\lambda_{\rm magic}$ as the wavelength where the ac polarizabilities of the two states are the same, leading to zero ac Stark shift for a corresponding transition.

For *np-ns* transitions considered in this work, it is found at the crossing of the ac polarizability curves for the *ns* and *np* states. In the case of the $np_{3/2}$-*ns* transitions, the magic wavelengths need to be determined separately for the cases with $m_j=\pm 1/2$ and $m_j=\pm 3/2$ owing to the presence of the tensor contribution to the total polarizability of $np_{3/2}$ state. According to Eq. (3), the total polarizability for the $np_{3/2}$ states is determined as $\alpha=\alpha_0-\alpha_2$ for $m_j=\pm 1/2$ and $\alpha=\alpha_0+\alpha_2$ for $m_j=\pm 3/2$. The uncertainties in the values of magic wavelengths are found as the maximum differences between the central value and the crossings of the $\alpha_{ns}\pm\delta\alpha_{ns}$ and $\alpha_{np}\pm\delta\alpha_{np}$ curves, where the $\delta\alpha$ are the uncertainties in the corresponding *ns* and *np* polarizability values.

We also study λ_{magic} for transitions between particular $np_{3/2}F'M'$ and *nsFM* hyperfine sublevels. The ac Stark shifts of the hyperfine sublevels of an atomic state are calculated using the method described in the previous section. In alkali-metal atoms, all magnetic sublevels have to be considered separately; therefore, a λ_{magic} is different for the $npF'M'$-*nsFM* transitions. We include several examples of such calculations.

We calculated the λ_{magic} values for $np_{1/2}$-*ns* and $np_{3/2}$-*ns* transitions for all alkali atoms from Na to Cs. As a general rule, we do not list the magic wavelengths which are extremely close to the resonances. Below, we discuss the calculation of the magic wavelengths separately for each atom. The figures are presented only for $np_{3/2}$ states as they are of more experimental relevance. All wavelengths are given in vacuum.

A. Na

We list the magic wavelengths λ_{magic} above 500 nm for the $3p_{1/2}$-3*s* and $3p_{3/2}$-3*s* transitions in Na and the corresponding values of polarizabilities at the magic wavelengths in Table III. For convenience of presentation, we also list the resonant wavelengths λ_{res} for transitions contributing to the $3p_{1/2}$ and $3p_{3/2}$ ac polarizabilities and the corresponding values of the electric-dipole matrix elements along with their uncertainties. Only two transitions contributing to the ground-state polarizabilities are above 500 nm, $3p_{1/2}$-3*s* and $3p_{3/2}$-3*s*. Therefore, there is no need to separately list resonant contributions to the ground-state polarizability. To indicate the placement of the magic wavelength, we order the lists of the resonant and magic wavelengths to indicate their respective placement. The polarizabilities and their uncertainties are calculated as described in Sec. II. The transitions up to *np*-3*s* and 3*p*-*nd*, $n=6$ are included into the main term and the remainder is evaluated in the DF approximation. The values of the 3*p*-3*s* matrix elements are taken from Ref. [18], the remaining matrix elements are either SD or SD scaled values. The uncertainties in the values of the Na matrix elements were estimated to be generally very small. The resonant wavelength values are obtained from energy levels from National Institute of Standards and Technology (NIST) database [9]. We assume no uncertainties in the energy values for all elements.

Since the 3*s* polarizability has only two resonant transitions at wavelengths greater than 500 nm, it is generally small except in close vicinity to those resonances. Since the polarizability of the $3p_{1/2}$ state has several contributions from the resonant transitions in this range, it is generally expected that it crosses the 3*s* polarizability in between of the each pair of resonances listed in Table III unless the wavelength is close to 3*p*-3*s* resonances. The same is expected in the case of the $3p_{3/2}$ polarizability for the $|m_j|=1/2$ cases as described by Eq. (3) ($\alpha=\alpha_0-\alpha_2$). However, when $\alpha=\alpha_0+\alpha_2$ [$m_j=\pm 3/2$ in Eq. (3)] all $3p_{3/2}$-*ns* transitions do not contribute to the total polarizability owing to the exact cancellation of the scalar and tensor contributions for $v=3p_{3/2}$ and $k=ns$ in Eqs. (4) and (5). In this case, the angular factor in Eq.(5) is exactly $-2/3(2j_v+1)$ leading to exact cancellation of such terms, and the total polarizability comes from the remaining 3*p*-*nd* contributions which do not cancel out. As a

TABLE III. Magic wavelengths λ_{magic} above 500 nm for the $3p_{1/2}$-3*s* and $3p_{3/2}$-3*s* transition in Na and the corresponding values of polarizabilities at the magic wavelengths. The resonant wavelengths λ_{res} for transitions contributing to the $3p_j$ ac polarizabilities and the corresponding absolute values of the electric-dipole matrix elements are also listed. The wavelengths (in vacuum) are given in nm and electric-dipole matrix elements and polarizabilities are given in atomic units.

Transition: $3p_{1/2}$-3*s*					
Resonances	d	λ_{res}		λ_{magic}	$\alpha(\lambda_{\text{magic}})$
$3p_{1/2}$-4*s*	3.576(1)	1138.46			
				1028.7(2)	241(1)
$3p_{1/2}$-$3d_{3/2}$	6.791	818.55			
				615.88(1)	1909(2)
$3p_{1/2}$-5*s*	0.757	615.59			
$3p_{1/2}$-3*s*	3.525(2)	589.76			
				589.457	52760(100)
$3p_{1/2}$-$4d_{3/2}$	1.917	568.42			
				566.57(1)	−1956(3)
$3p_{1/2}$-6*s*	0.391	515.03			
				514.72(1)	−514(1)
Transition: $3p_{3/2}m_j$-3*s*			$\lvert m_j\rvert$		
$3p_{3/2}$-4*s*	5.067(1)	1140.69			
			1/2	984.8(1)	252(1)
$3p_{3/2}$-$3d_{5/2}$	9.122(1)	819.71			
$3p_{3/2}$-$3d_{3/2}$	3.041	819.70			
			1/2	616.712(1)	1854(2)
$3p_{3/2}$-5*s*	1.071	616.25			
			1/2	589.636	−66230(80)
			3/2	589.557(1)	−42(2)
$3p_{3/2}$-3*s*	4.984(3)	589.16			
$3p_{3/2}$-$4d_{3/2}$	0.857	568.98			
$3p_{3/2}$-$4d_{5/2}$	2.571	568.98			
			1/2	567.43(1)	−2038(3)
			3/2	566.79(1)	−1976(3)
$3p_{3/2}$-6*s*	0.553	515.48			
			1/2	515.01(1)	−517(1)

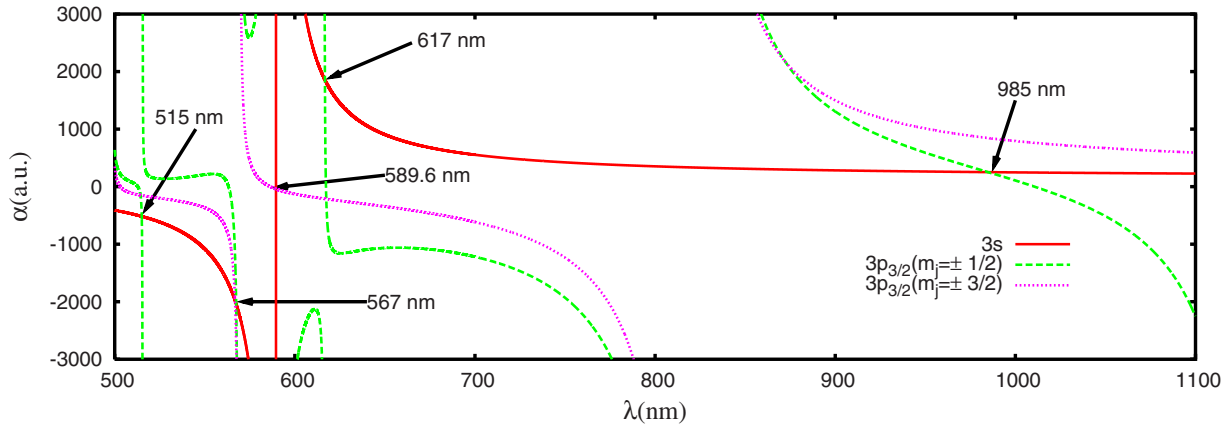

FIG. 1. (Color online) Frequency-dependent polarizabilities of Na atom in the ground and $3p_{3/2}$ states. The arrows show the magic wavelengths.

result, there are no resonances for the $m_j = \pm 3/2$ cases at the wavelengths corresponding to $3p_{3/2}$-ns transitions leading to substantial reduction in the number of magic wavelengths. We note that there is a magic wavelength at the 589.557 nm owing to the resonances in the ground-state polarizability. The corresponding polarizability value is very small making this case of limited practical use. While there has to be a magic wavelength between $3p_{3/2}$-$4d_{3/2}$ and $3p_{3/2}$-$4d_{5/2}$ resonances at 568.98 nm, we are not listing it owing to a very small value of the $4d$ fine-structure splitting. We illustrate the magic wavelengths for the $3p_{3/2}$-$3s$ transition in Fig. 1 where we plot the values of the ac polarizabilities for the ground and $3p_{3/2}$ states.

It is interesting to consider in more detail the region close to the $3p_j$-$3s$ resonances since in this case one magic wavelength is missing for both $3p_{1/2}$-$3s$ and $3p_{3/2}$-$3s$, α_0-α_2 cases, one on the side of each $3p$-$3s$ resonance as evident from Table III. We plot the ac polarizabilities for the $3s$, $3p_{1/2}$, and $3p_{3/2}m_j$ states in this region in Fig. 2. The placements of the $3p_{1/2}$-$3s$ and $3p_{3/2}$-$3s$ resonances are shown by vertical lines. In the case of the $3p_{1/2}$ state, the $3p_{1/2}$-$3s$ resonance contributes to both ground state and $3p_{1/2}$ polarizabilities. As a result, both of these polarizabilities are large but have opposite sign right of the $3p_{1/2}$-$3s$ resonance at 589.76 nm leading to missing magic wavelength for $3p_{1/2}$-$3s$ transition between the $3p_{1/2}$-$5s$ and $3p_{1/2}$-$3s$ resonances. In the $3p_{3/2}$-$3s$, $\alpha_0 - \alpha_2$ case, there is a missing magic wavelength to the left of the $3p_{3/2}$-$3s$ 589.12 nm resonance for the same reason. The values of the $\alpha_0 + \alpha_2$ for the $3p_{3/2}$ state are very small and negative in that entire region owing to the cancellations of the $3p$-$3s$ contributions in the scalar and tensor $3p_{3/2}$ polarizabilities described above.

In summary, there is only one case for Na in the considered range of the wavelengths where the magic wavelength exists for all sublevels (567 nm) at close values of the polarizabilities (−2000 a.u.) The ac polarizabilities for the $3s$ and $3p_{3/2}$ states near this magic wavelength are plotted in Fig. 3. The plot of the ac Stark shift for the transition between the hyperfine sublevels near 567 nm is shown in Fig. 4. The λ_{magic} is found at the point where the ac Stark shift of the transition from $3p_{3/2}F'=3M'$ sublevels to $3sFM$ sub levels crosses zero. This crossing of ac Stark shift curve occurs close to 567 nm which is close to the wavelength predicted by the crossing of polarizabilities illustrated by Fig. 3, as expected.

B. K

The magic wavelengths λ_{magic} above 600 nm for the $4p_{1/2}$-$4s$ and $4p_{3/2}$-$4s$ transitions in K are listed in Table IV.

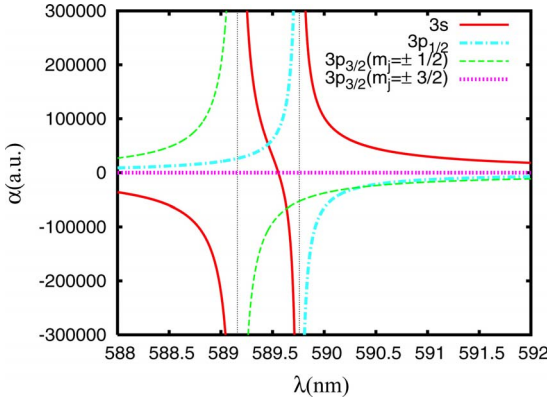

FIG. 2. (Color online) Magic wavelengths for the $3p_{1/2}$-$3s$ and $3p_{3/2}$-$3s$ transitions of Na.

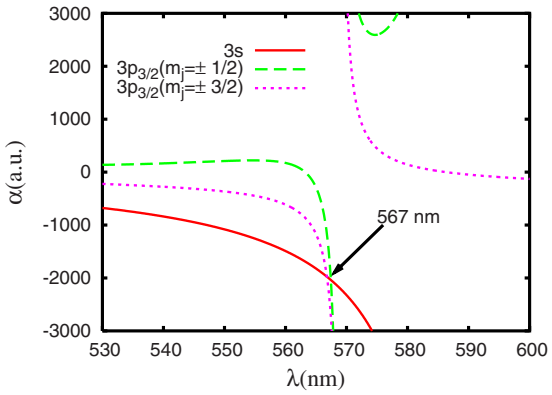

FIG. 3. (Color online) Magic wavelength for $3p_{3/2}$-$3s$ transition of Na.

TABLE IV. Magic wavelengths λ_{magic} above 600 nm for the $4p_{1/2}$-$4s$ and $4p_{3/2}$-$4s$ transition in K and the corresponding values of polarizabilities at the magic wavelengths. The resonant wavelengths λ_{res} for transitions contributing to the $4p_j$ ac polarizabilities and the corresponding absolute values of the electric-dipole matrix elements are also listed. The wavelengths (in vacuum) are given in nm and electric-dipole matrix elements and polarizabilities are given in atomic units.

Transition: $4p_{1/2}$-$4s$					
Resonances	d	λ_{res}	$\lvert m_j\rvert$	λ_{magic}	$\alpha(\lambda_{magic})$
$4p_{1/2}$-$5s$	3.885(19)	1243.57			
			1/2	1227.7(2)	472(1)
$4p_{1/2}$-$3d_{3/2}$	7.984(35)	1169.34			
$4p_{1/2}$-$4s$	4.102(5)	770.11			
			1/2	768.413(4)	20990(80)
$4p_{1/2}$-$4d_{3/2}$	0.097(57)	693.82			
$4p_{1/2}$-$6s$	0.903	691.30			
			1/2	690.15(1)	−1186(2)
Transition: $4p_{3/2}m_j$-$4s$			$\lvert m_j\rvert$		
$4p_{3/2}$-$5s$	5.535(26)	1252.56			
			1/2	1227.7(2)	472(1)
$4p_{3/2}$-$3d_{5/2}$	10.741(47)	1177.61			
$4p_{3/2}$-$3d_{3/2}$	3.580(16)	1177.29			
			1/2	769.432(2)	−27190(60)
			3/2	768.980(3)	−356(8)
$4p_{3/2}$-$4s$	5.800(8)	766.70			
$4p_{3/2}$-$4d_{5/2}$	0.10(15)	696.66			
$4p_{3/2}$-$4d_{3/2}$	0.033(47)	696.61			
$4p_{3/2}$-$6s$	1.279	694.07			
			1/2	692.32(2)	−1226(3)

Table IV is structured in exactly the same way as Table III. The electric-dipole matrix elements for the $4p$-$4s$ transitions are taken from Ref. [18], and the electric-dipole matrix elements for the $4p$-$3d$ are the recommended values from Ref. [22] derived from the accurate Stark shift measurements

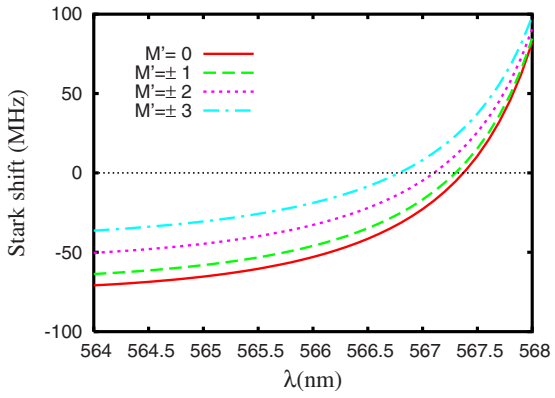

FIG. 4. (Color online) ac Stark shifts for the transition from $3p_{3/2}F'=3M'$ sublevels to $3sFM$ sublevels in Na as a function of wavelength. The electric field intensity is taken to be 1 MW/cm^2.

TABLE V. Magic wavelengths λ_{magic} above 600 nm for the $5p_{1/2}$-$5s$ transition in Rb and $6p_{1/2}$-$6s$ transitions in Cs and the corresponding values of polarizabilities at the magic wavelengths. The resonant wavelengths λ_{res} for transitions contributing to the np_j ac polarizabilities and the corresponding absolute values of the electric-dipole matrix elements are also listed. The wavelengths (in vacuum) are given in nm and electric-dipole matrix elements and polarizabilities are given in atomic units.

Rb Transition: $5p_{1/2}$-$5s$				
Resonances	d	λ_{res}	λ_{magic}	$\alpha(\lambda_{magic})$
$5p_{1/2}$-$4d_{3/2}$	8.051(67)	1475.65		
			1350.9(5)	476(1)
$5p_{1/2}$-$6s$	4.146(27)	1323.88		
$5p_{1/2}$-$5s$	4.231(3)	794.98		
			787.6(1)	5417(25)
$5p_{1/2}$-$5d_{3/2}$	1.35(7)	762.10		
			761.5(1)	−5230(30)
$5p_{1/2}$-$7s$	0.953(2)	728.20		
			727.35(1)	−1877(3)
$5p_{1/2}$-$6d_{3/2}$	1.07(11)	620.80		
			617.7(7)	−490(3)
$5p_{1/2}$-$8s$	0.502(2)	607.24		
			606.2(1)	−444(1)
Cs Transition: $6p_{1/2}$-$6s$				
$6p_{1/2}$-$5d_{3/2}$	7.016(24)	3011.15		
			1520(3)	583(2)
$6p_{1/2}$-$7s$	4.236(21)	1359.20		
$6p_{1/2}$-$6s$	4.489(7)	894.59		
$6p_{1/2}$-$6d_{3/2}$	4.25(11)	876.38		
$6p_{1/2}$-$8s$	1.026	761.10		
			759.40(3)	−1282(3)
$6p_{1/2}$-$7d_{3/2}$	2.05(2)	672.51		
			660.1(6)	−513(3)
$6p_{1/2}$-$9s$	0.548	635.63		
			634.3(2)	−424(2)
$6p_{1/2}$-$8d_{3/2}$	1.30(2)	601.22		

[26]. The resonant wavelengths are obtained from the energy levels compiled in the NIST database [9]. The transitions up to $4p$-$10s$ and $4p$-$9d$ are included into the main term of the polarizability, and the remainder is evaluated in the DF approximation. In the case of some higher states, such as $9s$, we did not evaluate the uncertainties of the matrix elements where we expect them to be small (below 0.5%). As a result, the uncertainties in the values of the magic wavelengths near these transitions do not include these contributions and may be slightly larger than estimated. In the test case of Rb, the uncertainties are evaluated for all transitions with resonant wavelengths above 600 nm and no significant differences in the uncertainties of the relevant magic wavelengths with other elements are observed.

The main difference between the Na and K calculation is the extremely large correlation correction to the values of the

TABLE VI. Magic wavelengths λ_{magic} above 600 nm for the $5p_{3/2}$-$5s$ transition in Rb and $6p_{3/2}$-$6s$ transitions in Cs and the corresponding values of polarizabilities at the magic wavelengths. The resonant wavelengths λ_{res} for transitions contributing to the np_j ac polarizabilities and the corresponding absolute values of the electric-dipole matrix elements are also listed. The wavelengths (in vacuum) are given in nm and electric-dipole matrix elements and polarizabilities are given in atomic units.

Rb Transition: $5p_{3/2}m_j$-$5s$			$\lvert m_j\rvert=1/2$		$\lvert m_j\rvert=3/2$	
Resonances	d	λ_{res}	λ_{magic}	$\alpha(\lambda_{magic})$	λ_{magic}	$\alpha(\lambda_{magic})$
$5p_{3/2}$-$4d_{5/2}$	10.90(9)	1529.37				
$5p_{3/2}$-$4d_{3/2}$	3.63(3)	1529.26				
			1414.8(5)	456(1)		
$5p_{3/2}$-$6s$	6.05(3)	1366.87				
			792.00(1)	−6910(30)	789.98(2)	125(35)
$5p_{3/2}$-$5s$	5.977(4)	780.24				
$5p_{3/2}$-$5d_{3/2}$	0.67(3)	776.16				
$5p_{3/2}$-$5d_{5/2}$	1.98(9)	775.98				
			775.84(1)	−19990(70)	775.77(3)	−19700(130)
$5p_{3/2}$-$7s$	1.350(2)	741.02				
			740.07(1)	−2494(4)		
$5p_{3/2}$-$6d_{3/2}$	0.51(5)	630.10				
$5p_{3/2}$-$6d_{5/2}$	1.51(15)	630.01				
			627.3(5)	−533(4)	626.2(9)	−528(5)
$5p_{3/2}$-$8s$	0.708(2)	616.13				
			614.7(1)	−477(1)		
Cs Transition: $6p_{3/2}m_j$-$6s$			$\lvert m_j\rvert=1/2$		$\lvert m_j\rvert=3/2$	
$6p_{3/2}$-$5d_{3/2}$	3.166(16)	3614.09				
			3611.8(2)	422(1)	3589(1)	422(1)
$6p_{3/2}$-$5d_{5/2}$	9.59(8)	3490.97				
			1910(6)	498(2)		
$6p_{3/2}$-$7s$	6.47(3)	1469.89				
			932.4(8)	3197(50)	940.2(1.7)	2810(70)
$6p_{3/2}$-$6d_{3/2}$	2.10(5)	921.11				
			921.01(3)	4088(10)	920.18(6)	4180(14)
$6p_{3/2}$-$6d_{5/2}$	6.15(14)	917.48				
			887.95(10)	−5600(100)	883.4(2)	−1550(90)
$6p_{3/2}$-$6s$	6.324(7)	852.35				
$6p_{3/2}$-$8s$	1.461	794.61				
			793.07(2)	−2074(5)		
$6p_{3/2}$-$7d_{3/2}$	0.976(9)	698.54				
			698.524(2)	−697(2)	698.346(4)	−696(2)
$6p_{3/2}$-$7d_{5/2}$	2.89(3)	697.52				
			687.3(3)	−635(3)	684.1(5)	−618(4)
$6p_{3/2}$-$9s$	0.770	658.83				
			657.05(9)	−500(1)		
$6p_{3/2}$-$8d_{3/2}$	0.607(8)	621.93				
			621.924(2)	−388(1)	621.844(3)	−388(1)
$6p_{3/2}$-$8d_{5/2}$	1.81(2)	621.48				
			615.5(8)	−371(3)	614(3)	−367(8)
$6p_{3/2}$-$10s$	0.509	603.58				
			602.6(4)	−339(1)		

$4p$-$4d$ transitions. The correlation correction nearly exactly cancels the lowest-order DF value leading to a value that is essentially zero within the accuracy of this calculation. As a result, we do not quote the values for the magic wavelength between $4p$-$4d$ and $4p$-$6s$ resonances. We note that these two resonances are very closely spaced (1.5 nm), thus probably making the use of such a magic wavelength impractical. Our present calculation places the magic wavelength for the $4p_{1/2}$-$4s$ transition in the direct vicinity (within 0.01 nm) of the 693.82 nm resonance. We note that the measurement of the ac Stark shift (or the ratio of the $4s$ to $4p$ Stark shifts) near the $4p$-$4d$ resonance may provide an excellent benchmark test of atomic theory. This problem of the cancellation of the lowest and higher-order terms for the *np-nd* transitions is unique to K. In the case of Rb, the correlation for the similar $5p$-$5d$ transition is very large but adds coherently to the DF values. As a result, we were able to evaluate the corresponding Rb $5p$-$5d$ matrix elements with 4.5% accuracy. The accuracy is further improved for the $6p$-$6d$ transitions in Cs.

We also located the magic wavelengths for the $4p_{3/2}$-$4s$ transition between $4p_{3/2}$-$3d_{3/2}$ and $4p_{3/2}$-$3d_{5/2}$ resonances, but found that $m_j=\pm 1/2$ curve crosses the $4s$ polarizability very close (within 0.002 nm) to the resonance. Therefore, we do not list this crossing in Table IV. We note that $m_j=\pm 3/2$ curve crosses the $4s$ polarizability curve further away from resonance at 1177.35 nm. The polarizability values for both of these crossings is 500 a.u.

C. Rb

We list the magic wavelengths λ_{magic} above 600 nm for the $5p_{1/2}$-$5s$ transition in Rb and the $6p_{1/2}$-$6s$ transition in Cs in Table V. In this case, all Rb $5p_{1/2}$-nl_j resonances have significant spacing allowing us to determine the corresponding magic wavelengths. The magic wavelengths above 600 nm for the $5p_{3/2}$-$5s$ transition in Rb and $6p_{3/2}$-$6s$ transition in Cs are grouped together in Table VI. The transitions up to $5p$-$10s$ and $5p$-$9d$ are included in the main term calculation of the Rb $5p$ polarizabilities and the remainder is evaluated in the DF approximation. The $5p$-$5s$ matrix elements are taken from Ref. [18], and the $5p$-$4d$ $E1$ matrix elements are the recommended values derived from the Stark shift measurements [26] in Ref. [22]. As we discussed in Sec. II, the correlation correction is very large for the $5p$-$5d$ transitions; the DF values for the $5p_{3/2}$-$5d_{5/2}$ transition is 0.5 a.u. while our final value is 2 a.u.. However, nearly entire correlation correction to this value comes from the single all-order term which can be more accurately estimated by the scaling procedure described in Refs. [8,15,16]. To evaluate the uncertainty of these values, we also conducted another calculation including the triple excitations relevant to the correction of the dominant correlation term (SDpT method), and repeated the scaling procedure for the SDpT calculation. We took the spread of the final values and the SDpT *ab initio* and SDpT scaled values to be the uncertainty of the final numbers. Nevertheless, even such an elaborate calculation still gives an estimated uncertainty of 4.5%.

We illustrate the λ_{magic} for the $5p_{3/2}$-$5s$ transition near 791 nm in Fig. 5. We note that this case is different from that

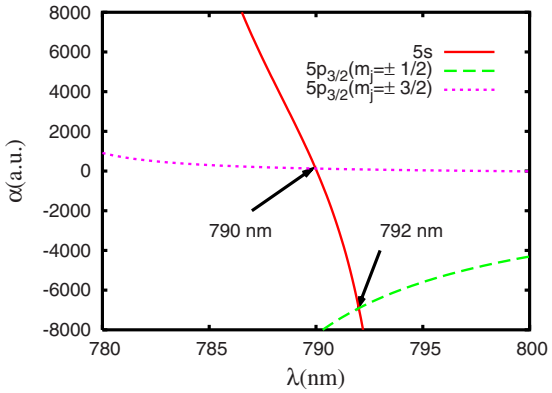

FIG. 5. (Color online) Magic wavelengths for the $5p_{3/2}$-$5s$ transition of Rb.

of Na illustrated in Fig. 3, where both $\alpha_0+\alpha_2$ and $\alpha_0-\alpha_2$ curves for the $3p_{3/2}$ polarizability cross the $3s$ polarizability curve at approximately the same polarizability values. In the Rb case near 791 nm, $\alpha_0+\alpha_2$ and $\alpha_0-\alpha_2$ curves for the $5p_{3/2}$ polarizability cross the $5s$ polarizability curve at 125 and −6910 a.u., respectively. As a result, the $|M'|=3$ curve on the ac Stark shift plot for the transition between hyperfine sub levels shown in Fig. 6 is significantly split from the curves for the other sublevels.

The magic wavelengths for the $5p_{3/2}$-$5s$ transition between the fine-structure components of the $5p$-nd_j levels are not listed owing to very small fine structures of these levels. We note that crossings for all m_j sublevels should be present between the fine-structure components of the $5p$-nd_j lines. We illustrate such magic wavelengths for Cs, which has substantially larger nd_j fine-structure splittings.

D. Cs

Our results for Cs are listed in Tables V and VI. The values of the $6p$-$6s$ matrix elements are taken from Ref. [35], and the values for $6p$-$7s$ transitions are taken from the results compiled in Ref. [15] (derived from the $7s$ lifetime value). We derived the $6p_{1/2}$-$5d_{3/2}$ value from the experimental value

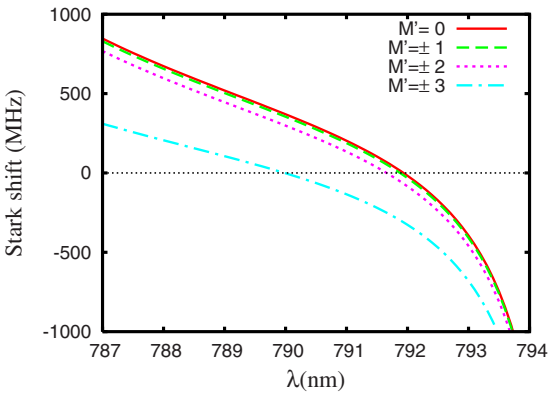

FIG. 6. (Color online) ac Stark shifts for the transition from $5p_{3/2}F'=3M'$ sublevels to $5sFM$ sublevels in Rb as a function of wavelength. The electric field intensity is taken to be 1 MW/cm^2.

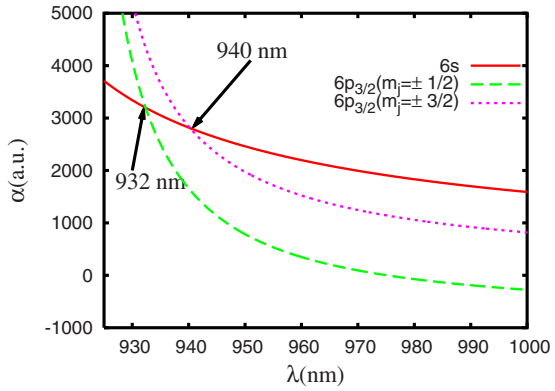

FIG. 7. (Color online) Polarizability of the $6p_{3/2}$ state and polarizability of ground state of Cs as a function of wavelength. Magic wavelengths for the $6p_{3/2}$-$6s$ transition of Cs are found to be at 932 and 940 nm depending on the m_j value.

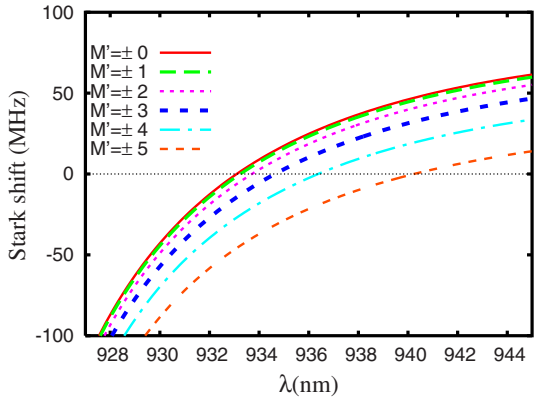

FIG. 8. (Color online) ac Stark shifts for the transition from $6p_{3/2}F'=5M'$ sublevels to $6sFM$ sublevels in Cs as a function of wavelength. The electric field intensity is taken to be 1 MW/cm^2.

of the $D1$ line Stark shift in Cs [21] combined with the experimental ground-state polarizability value from Ref. [30]. The procedure for deriving the matrix element values from the Stark shifts is described in Ref. [22]. We use the theoretical values of the ratios of the $6p_{1/2}$-$5d_{3/2}$, $6p_{3/2}$-$5d_{3/2}$, and $6p_{3/2}$-$5d_{5/2}$ values from Ref. [8] to obtain the values for the $6p_{3/2}$-$5d_{3/2}$ and $6p_{3/2}$-$5d_{5/2}$ matrix elements. We use the experimental energy levels from Refs. [10,11,36], and references therein to obtain the resonance wavelength values. The transitions up to $6p$-$12s$ and $6p$-$9d$ are included into the main term calculation of the polarizabilities and the remainder is evaluated in the DF approximation.

We find that there are no magic wavelengths for the $6p_{1/2}$-$6s$ transition in between the $6p_{1/2}$-$6s$, $6p_{1/2}$-$6d_{3/2}$, and $6p_{1/2}$-$8s$ resonances whereas there are the magic wavelengths in between the corresponding resonances in Rb. The difference between the Rb and Cs cases is in the placement of the $6p_{3/2}$-$6s$ resonance in Cs and $5p_{3/2}$-$5s$ resonance in Rb. In Rb, $5p_{3/2}$-$5s$ resonance is at 780 nm and follows the $5p_{1/2}$-$5s$ one. In Cs, the $6p_{3/2}$-$6s$ resonance is at 852 nm and is located in between the $6p_{1/2}$-$6d_{3/2}$ and $6p_{1/2}$-$8s$ resonances owing to much larger $6p$ fine-structure splitting. As a result, there are no magic wavelengths in this range.

Also unlike the Rb case, the magic wavelengths around 935 nm for the $6p_{3/2}$-$6s$ transition in Cs correspond to similar values of the polarizability (about 3000 a.u.) for all sublevels as illustrated in Fig. 7. The nearest resonances to this magic wavelength are $6p_{3/2}$-$6d_j$ ones; therefore the contributions from these transitions are dominant. To improve the accuracy of these values, we conducted a more accurate calculation for these transitions following the $5p$-$5d$ Rb calculation described in the previous subsection. As a result, we expect our values of the $6p$-$6d$ matrix elements to be more accurate than the one quoted in Ref. [8]. Nevertheless, the uncertainties in the values of the corresponding magic wavelengths are quite high because the $6s$ and $6p_{3/2}$ polarizability curves cross at very small angles. As a result, even relatively small uncertainties in the values of the polarizabilities propagate into significant uncertainties in the values of the magic wavelengths. Our values for these magic wavelengths are in good agreement with previous studies [3,37,38]. The ac Stark shift of the $6p_{3/2}F'=5M'$ to $6sFM$ transition as a function of wavelength at the 925–945 nm range is plotted in Fig. 8.

V. CONCLUSION

We have calculated the ground ns state and np state ac polarizabilities in Na, K, Rb, and Cs using the relativistic all-order method and evaluated the uncertainties of these values. The static polarizability values were found to be in excellent agreement with previous experimental and theoretical results. We have used our calculations to identify the magic wavelengths at which the ac polarizabilities of the alkali-metal atoms in the ground state are equal to the ac polarizabilities in the excited np_j states facilitating state-insensitive cooling and trapping.

ACKNOWLEDGMENTS

We gratefully acknowledge helpful discussions with Fam Le Kien. This work was performed under the sponsorship of the National Institute of Standards and Technology, U.S. Department of Commerce.

[1] D. Jaksch, H. J. Briegel, J. I. Cirac, C. W. Gardiner, and P. Zoller, Phys. Rev. Lett. **82**, 1975 (1999).

[2] H. Katori, T. Ido, and M. Kuwata-Gonokami, J. Phys. Soc. Jpn. **68**, 2479 (1999).

[3] J. McKeever, J. R. Buck, A. D. Boozer, A. Kuzmich, H.-C. Nagerl, D. M. Stamper-Kurn, and H. J. Kimble, Phys. Rev. Lett. **90**, 133602 (2003).

[4] J. R. P. Angel and P. G. H. Sandars, Proc. R. Soc. London, Ser.

A **305**, 125 (1968).
[5] R. W. Schmieder, Am. J. Phys. **40**, 297 (1972).
[6] D. Budker, D. F. Kimball, and D. R. DeMille, *Atomic Physics: An Exploration Through Problems and Solutions* (Oxford University Press, Oxford, 2004).
[7] W. R. Johnson, D. Kolb, and K.-N. Huang, At. Data Nucl. Data Tables **28**, 334 (1983).
[8] M. S. Safronova and C. W. Clark, Phys. Rev. A **69**, 040501(R) (2004).
[9] Y. Ralchenko, F. C. Jou, D. E. Kelleher, A. E. Kramida, A. Musgrove, J. Reader, W. L. Wiese, and K. Olsen, *NIST Atomic Spectra Database*, 2005, version 3.1.2 (online). Available at http://physics.nist.gov/asd3 (2007, August 29). National Institute of Standards and Technology, Gaithersburg, MD.
[10] C. E. Moore, *Atomic Energy Levels*, NSRDS–NBS 35 (U.S. Government Printing Office, Washington, D.C., 1971).
[11] J. Sansonetti, W. Martin, and S. Young, *Handbook of Basic Atomic Spectroscopic Data*, 2005, version 1.1.2 (Online). Available at http://physics.nist.gov/Handbook (2007, August 29). National Institute of Standards and Technology, Gaithersburg, MD.
[12] S. G. Porsev, Y. G. Rakhlina, and M. G. Kozlov, Phys. Rev. A **60**, 2781 (1999).
[13] M. S. Safronova, B. Arora, and C. W. Clark, Phys. Rev. A **73**, 022505 (2006).
[14] S. A. Blundell, W. R. Johnson, Z. W. Liu, and J. Sapirstein, Phys. Rev. A **40**, 2233 (1989).
[15] M. S. Safronova, W. R. Johnson, and A. Derevianko, Phys. Rev. A **60**, 4476 (1999).
[16] S. A. Blundell, W. R. Johnson, and J. Sapirstein, Phys. Rev. A **43**, 3407 (1991).
[17] M. S. Safronova, C. J. Williams, and C. W. Clark, Phys. Rev. A **69**, 022509 (2004b).
[18] U. Volz and H. Schmoranzer, Phys. Scr., T **65**, 48 (1996).
[19] A. Kreuter, *et al.*, Phys. Rev. A **71**, 032504 (2005).
[20] M. Gunawardena, D. S. Elliott, M. S. Safronova, and U. Safronova, Phys. Rev. A **75**, 022507 (2007).
[21] L. R. Hunter, J. D. Krause, K. E. Miller, D. J. Berkeland, and M. G. Boshier, Opt. Commun. **94**, 210 (1992).
[22] B. Arora, M. S. Safronova, and C. W. Clark (unpublished).
[23] C. Zhu, A. Dalgarno, S. G. Porsev, and A. Derevianko, Phys. Rev. A **70**, 032722 (2004).
[24] C. R. Ekstrom, J. Schmiedmayer, M. S. Chapman, T. D. Hammond, and D. E. Pritchard, Phys. Rev. A **51**, 3883 (1995).
[25] L. Windholz and M. Musso, Phys. Rev. A **39**, 2472 (1989).
[26] K. E. Miller, D. Krause, and L. R. Hunter, Phys. Rev. A **49**, 5128 (1994).
[27] A. Derevianko, W. R. Johnson, M. S. Safronova, and J. F. Babb, Phys. Rev. Lett. **82**, 3589 (1999).
[28] C. Krenn, W. Scherf, O. Khait, M. Musso, and L. Windholz, Z. Phys. D: At., Mol. Clusters **41**, 229 (1997).
[29] W. van Wijngaarden and J. Li, J. Quant. Spectrosc. Radiat. Transf. **52**, 555 (1994).
[30] J. M. Amini and H. Gould, Phys. Rev. Lett. **91**, 153001 (2003).
[31] C. E. Tanner and C. Wieman, Phys. Rev. A **38**, 162 (1988).
[32] L. Windholz and C. Neueiter, Phys. Lett. **109A**, 155 (1985).
[33] T. A. Birks, W. J. Wadsworth, and P. S. J. Russell, Opt. Lett. **25**, 1415 (2000).
[34] Daniel A. Steck, Alkali D Line Data, URL: http://steck.us/alkalidata/
[35] R. J. Rafac, C. E. Tanner, A. E. Livingston, and H. G. Berry, Phys. Rev. A **60**, 3648 (1999).
[36] K.-H. Weber and C. J. Sansonetti, Phys. Rev. A **35**, 4650 (1987).
[37] F. L. Kien, V. I. Balykin, and K. Hakuta, J. Phys. Soc. Jpn. **74**, 910 (2005).
[38] Yu-Nan Zheng, Xiao-Ji Zhou, and Xu-Zong Chen, Chin. Phys. Lett. **23**, 1687 (2006).